Sov. Lightwave Commun. 3 (1993) 91–100. Printed in the UK

790

# Femtosecond passively mode-locked Yb–Er fibre laser

A B Grudinin, I Yu Khrushchev and A V Kuznetsov

General Physics Institute, Russian Academy of Sciences, 38 Vavilov Street, 117942, Moscow, Russia

Received 24 February 1993, in final form 6 April 1993

**Abstract.** We present here results of an experimental study of temporal and spectral characteristics of the Figure-8 laser. The laser itself produces 850 fs bandwidth-limited pulses. Exploitation of a dispersion-shifted fibre at the laser output results in compression of the laser pulses to 250 fs.

## 1. Introduction

In recent years much work has been devoted to the development of erbium-doped fibre lasers, because a broad gain bandwidth centred near 1.54 $\mu$m, negative group velocity dispersion and tight confinement of optical field allow the exploitation of nonlinear optical effects for very effecient generation of ultra-short optical pulses.

In the last few years several mode-locked schemes exploiting fibre nonlinearity have been reported [1–8]. In fact there are two main types of mode-locked fibre lasers: schemes which require active modulation in order to initiate mode-locking with successive pulse sharpening using the Kerr effect in optical fibres [1–3] and pure passive mode-locked schemes, based on nonlinear optical switch effect [4–8].

Passive generation of femtosecond pulses in erbium-doped fibre lasers has recently become of considerable interest. The Figure-8 laser configuration [4] whose operation is based on the reflection properties of the Nonlinear Amplifying Loop Mirror (NALM) [9] has been the object of considerable study [4–8, 10, 11]. Although the general principle of operation of the Figure-8 laser is understood many features of its behaviour still remain to be adequately investigated and explained.

In particular, the absence of the modulator within the cavity of a passively mode-locked fibre laser results in some uncertainity in the temporal position of the travelling pulse. Moreover in the case of propagation of several pulses within the cavity the time interval between pulses becomes a random value since there is no force keeping the pulses at well-defined distance. As a result, interaction between pulses through different effects causes complicated behaviour of the laser output. As has been pointed out by several authors the Figure-8 laser may operate in several regimes producing either clean soliton-like or 'square' pulses [11]. Usually temporal measurements are fulfilled by autocrrelation technique which possessing a high temporal resolution does not allow to conclude directly about cleanliness (i.e. existence of double pulses, satellites etc) of the generated pulses. From this point of view the exploitation of a streak camera with resolution of $\sim$ 1 ps can bring additional information about capabilities of the Figure-8 laser.

In this paper we present the results of experimental study of temporal and spectral characteristics of the Figure-8 laser based on codoped Yb–Er fibre. In temporal

0960-0884/93/020091+10$07.50  

measurements we have used both a streak camera and autocorrelator carring out measurements at different pump power levels. We show that by a suitable choice of laser parameters (pump power and reflectivity of the output coupler) one can compress output pulses to generate clean, bandwidth-limited femtosecond pulses.

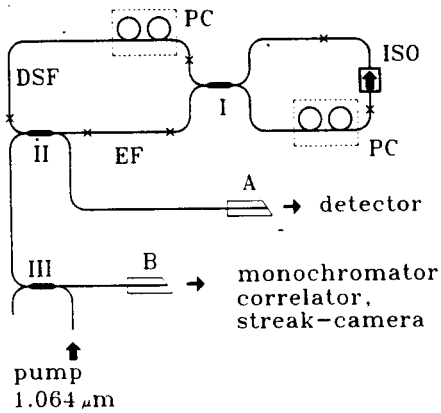


**Figure 1.** Experimental configuration: PC, polarization controllers; ISO, optical isolator; EF, codoped Yb–Er fibre; DSF, dispersion-shifted fibre of 35 m length; I, 3 dB coupler; II and III are WDMs (for details see text).

## 2. Experimental results

The experimental setup is shown in figure 1. The experimental configuration employed a loop coupler arranged to give 50:50 coupling at 1560 nm. The unidirectional loop consists of a polarization dependent isolator, a 3 m length of single-mode fibre and polarization control discs (PCs). The effective NALM length was 25 m and the total cavity length was 35 m, corresponding to a fundamental frequency of about 6 MHz. Fibre dispersion $D = -3.2$ ps nm$^{-1}$ km$^{-1}$ and effective mode area $A_{\text{eff}} = 35$ $\mu$m at 1560 nm. The amplifier section consists of 4 m of codoped fibre with Yr and Er ion concentration of 5000 ppm and 800 ppm respectively. Pump power was launched through a wavelength division multiplexer (WDM) II (0.43 output coupling at 1560 nm) and III (1.0 at 1560 nm). Such a configuration of the laser allows us to measure simultaneously energy of pulses travelling in opposite directions around NALM and by this way to estimate saturated gain of the laser.

Since we have used polarization-non-preserving fibres with polarization beat length of a few metres than the vital elements of the present configutarion were PCs. Rotation of PCs placed in the NALM introduces phase bias into cavity-loss characteristic resulting in non-zero transmission of the loop coupler in the linear regime and that in turn increases the system's ability to self-start.

Temporal characteristics of the output radiation were taken in real time by a streak camera with temporal resolution better than 1.5 ps at 1560 nm and using a background-free autocorrelator. Calibrated photodiodes were used for the laser gain measurements.

A typical laser output characteristic measured at port A is shown in figure 2 and exibits jumps and hysteresis in the output power assosiated with energy quantization in fibre soliton lasers [11]. The dependence of gain against the pump power was also measured. Figure 3 shows the saturated gain $G$ as a function of the pump power. The gain and, hence, the

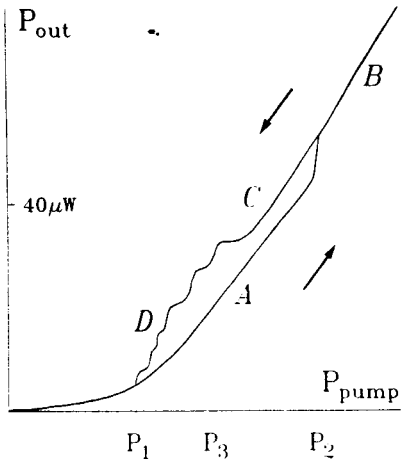


**Figure 2.** Laser output $P_A$ against launched pump power.

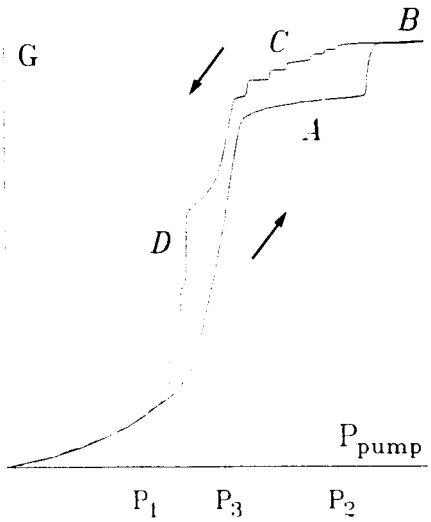


**Figure 3.** Saturated gain $G$ against launched pump power.

losses in the cavity are maximal under low pump level. The gain decreased with rising pump power and had a jump from 20 to 17 at the start point.

Note the qualitatively different behaviour of the laser output at different pump power levels. At the point of 'second threshold' $P_2$, when the passive mode-locked process self-starts, the number of pulses $N$ circulating within the cavity equals 20–50. Usually pulses are bundled together within a 10–100 ns time interval. A few pulses from the group undergo chaotic motion within the nanosecond time interval while the rest are fixed and motionless. Increasing pump power results in a more progressive motion of pulses and at $P_{\text{pump}} \approx 1.1P_2$ at the scope screen we observed only a nanosecond envelope without any distinctive pulses within it. As the pump power is lowered below the self-starting threshold the pulse motions become less chaotic and than the pulses group themselves into ordered patterns and all motions cease. As the pump power is further reduced abrupt jumps in output power are observed and are associated with the disappearance of individual pulses from the pulse train. Note that the time interval in the motionless pattern was usually equal to a few nanoseconds and we have never seen a stable pattern with a picosecond time scale interval.

By measuring the change in output power during individual pulse disappearance we estimated the energy of pulses circulating within the nonlinear loop in both directions. In point $P_3$ of figure 2 one has $E_+ = 27$ pJ for a clockwise-propagating pulse while for a counter-propagating pulse, $E_- = 2.1$ pJ, which gives us a saturated laser gain at this point (taking into account output coupling) as $G = 21$.

## 3. Discussion

### *3.1. Single multisoliton pulse generation and compression*

Laser temporal characteristics strongly depend on pump power. Being pumped by a relatively low power (region D in figure 2), the laser generated few single unmovable soliton-like pulses (figure 4(*A*)). The pulses were of 850 fs duration and were close to

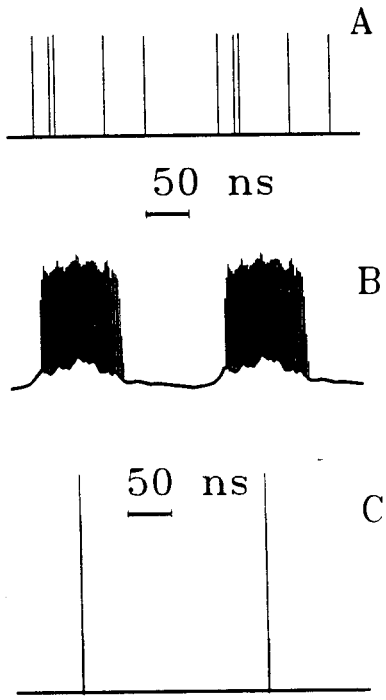


**Figure 4.** Oscilloscope traces of: (*a*) single soliton pulses, (*b*) soliton bunches, (*c*) noise pulses.

bandwidth-limited ones (see figures 6(*A*) and (*B*)). In the simplest model [5] the duration of the solitons generated is related with the laser parameters through the expression

$$\tau^2 = \left(\frac{0.776\lambda^2}{\pi^2 c n_2}\right) DL(G-1) \tag{1}$$

where $n_2$ is a nonlinear refractive index, $D$ is dispersion of the NALM fibre and $L$ is the effective NALM lengh. In our laser output coupler II is situated in the NALM near the active fibre (see figure 1) and the nonlinear phase of an amplified pulse in the NALM is related to the effective gain coefficient $\tilde{G} = G(1-\gamma_{\text{out}}) = 1/\alpha$ where $\gamma_{\text{out}}$ is the output coupling coefficient and $\alpha$ is the linear loop transmission. The gain coefficient $G$ in (1) must be replaced by $\tilde{G}$ for this laser scheme. Substituting in (1) the laser parameters taken in point $P_3$ (see figures 2 and 3) we obtain a duration of 750 fs that is in relatively good agreement with the experimental value of 850 fs. There is to note, that the output pulse duration in this approximation does not depend on the output coupling coefficient but its power is about

$$P_{\text{out}} = \frac{P_{\text{in}}\gamma}{2\alpha(1-\gamma)} \tag{2}$$

where $P_{\text{in}}$ is the pulse power at the NALM input which is about the fundamental soliton power. In the experiment we have observed at the laser output pulses of 850 fs duration and of 21 W peak power. It was possible to compress the pulses in the additional dispersion-shifted fibre to 250 fs (see figures 6 and 7 below). The change of the output coupling coefficient from 0.43 to 0.9 (by replacing the coupler) had no effect on the generated pulses duration and spectrum. The output power increasing by rising the output coupling should be limited by the gain characteristics of active fibre and by soliton effects in this fibre. Nevertheless, our laser configuration (figure 1) allows us to generate multisoliton subpicosecond pulses.

### *3.2. Soliton bunches and noise pulse generation*

At high pump power level (regions $B$ and $C$ in figures 2 and 3) the laser generated bunches of solitons (figure 4($B$)) or soliton noise pulses (figure 4($C$)). Bunches consisted typically of 20–50 solitons including stable and moving ones. The ACF contrast and spectrum shapeform of soliton bunches was the same as that of single solitons at point $P_3$ of figures 2 and 3. The duration was between 850 and 750 fs. Pulses are bundled together within a 10–100 ns time interval. Increasing pump power results in a narrowing of the bunch and at $P_{\text{pump}} \approx 1.1P_2$ we observed only a nanosecond envelope without any distinctive pulses within it. The energy under the envelope fluctuated within ±15%. The real time streak-camera pictures showed the noise structure within 200 ps interval (figure 5).

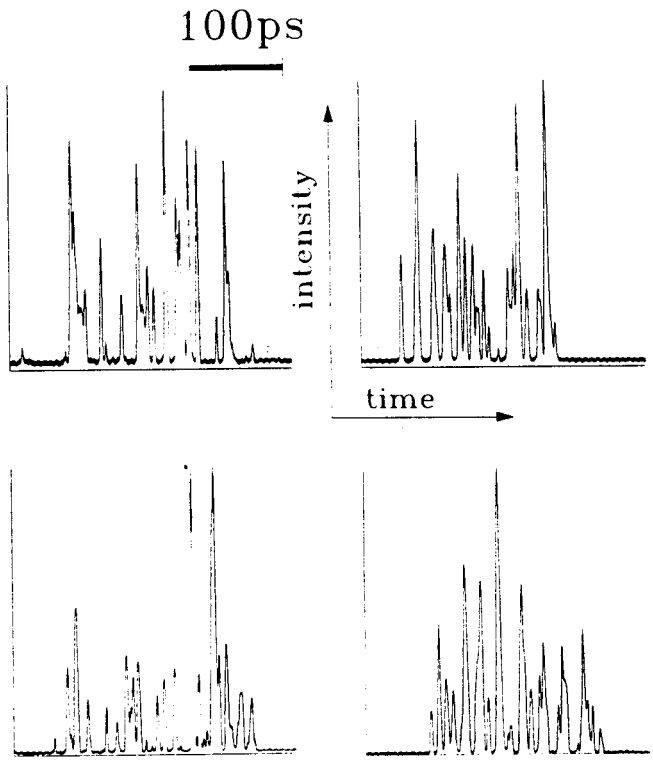


**Figure 5.** Streak-camera traces of noise pulses.

The structure and properties of these pulses are similar to those of Raman solitons, which appear under cascade Raman scattering in the anomalous dispersion region of optical fibre [12]. The noise pulses have relatively high contrast of ACF, random distance between solitons inside the pulse and hence, strong interaction between them. Solitons of the noise pulse can be compressed in exactly the same way, as clean single solitons (figures 6 and 7). The reason for formation of bunches and noise-pulses is not clear. A few mechanisms could be responsible for this phenomenon. One is the change in gain spectrum due to a saturation effect. If neighbouring pulses or groups of pulses are amplifying under different saturation circumstances their spectra, and hence their group velocities differ slightly one from another. Another possible mechanism of pulse attraction or repulsion is acousto-optical interaction—a weak effect, appearing under long-distance soliton propagation [13].

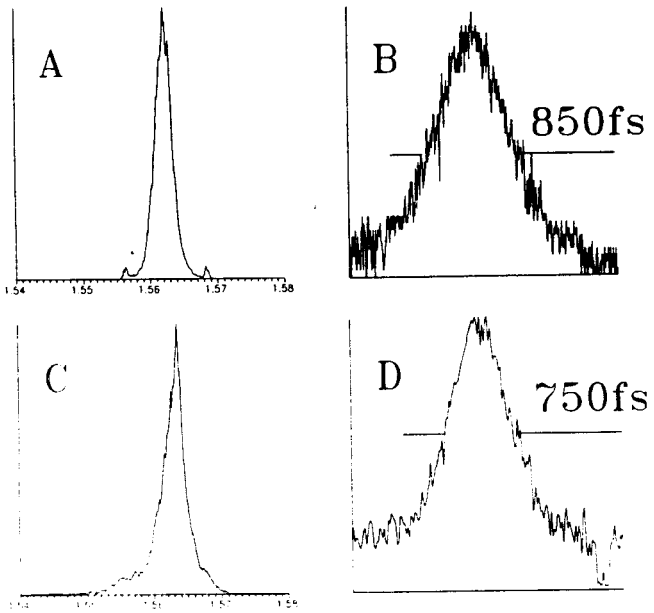


**Figure 6.** Spectra and ACF of soliton pulses (*A*, *B*) and those of noise pulses (*C*, *D*) at the laser output.

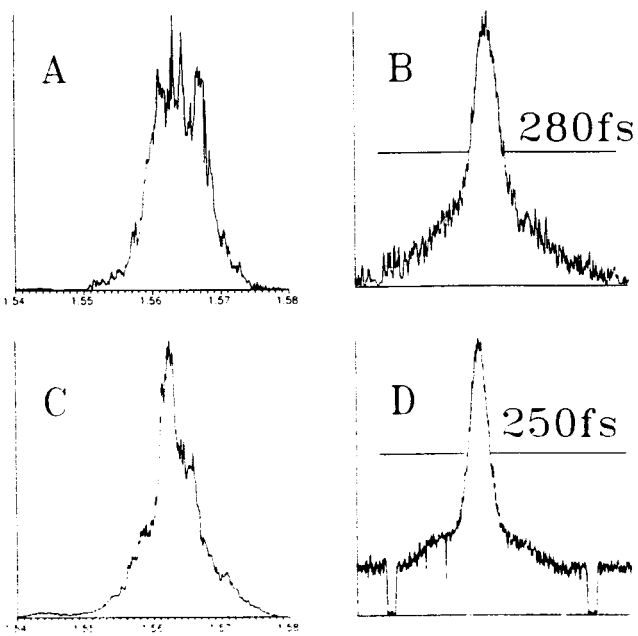


**Figure 7.** Spectra and ACF of soliton pulses (*A*, *B*) and that of noise pulses (*C*, *D*) after the dispersion-shifted fibre.

### *3.3. Mode-locking start conditions*

The Figure-8 laser is in fact a kind of additive-pulse mode-locking scheme (APM) and is analogous to lasers with a fast saturable absorber. A number of papers were recently devoted to the analysis of APM schemes [14, 15]. Unfortunately the Figure-8 laser differs from other APM lasers in that it does not allow us to use the standard approach of small changes of the pulse during the round-trip since the basic Figure-8 configuration incorporates a 50:50 coupler and a length of nonlinear loop, comparable with the period of solitons generated. Nontheless, some elements of the APM analysis are appropriate to our case. Here we apply the consideration of the mode-locking self-start in APM lasers to the Figure-8 laser.

It was shown [15] that the starting condition for the APM laser is

$$\frac{K}{G} > \sigma\beta\tau \tag{3}$$

where $G$ is a saturated gain, $\sigma$ the active medium cross-section, $\tau$ duration of the seeding pulse, $\beta$ the normalizing coefficient depending on the pulse shapeform and $K$ the proportional coefficient, relating dynamical transmission increase $\Delta G_s$ with the photon flux disturbance $\Delta F$:

$$K = \frac{\Delta G_n}{\Delta F}. \tag{4}$$

The photon flux disturbance caused by a pulse of power $P$ is

$$\Delta F = \frac{P}{h\nu A_{\text{eff}}}. \tag{5}$$

The main consideration involved is that the start of the laser is successful or, in other words, the seeding pulse survives, if the effective gain increase stemming from the nonlinear switching of the seeding pulse exceeds the gain saturation caused by this pulse

$$\Delta G_n - \Delta G_s > 0. \tag{6}$$

Under this circumstance the initial pulse grows at the first stage of the mode-locking. The value of $G_n$ depends on the laser configuration and in the Figure-8 laser it is simply equal to the NALM transmission of the seeding pulse

$$\Delta G_n = T = \frac{G}{2}(1 - \cos\phi_{\text{nl}}) \tag{7}$$

for the NALM with a 50:50 coupler. $\phi_{\text{nl}}$ is a nonlinear phase difference of the seeding pulse in the NALM. For $\phi_{\text{nl}} \ll \pi$ one can approximate $1 - \cos\phi \approx \phi^2/2$ and

$$\Delta G_n \approx \frac{G}{4}\phi_{\text{nl}}^2 \tag{8}$$

In the critical point ($G_n = G_s$ coefficient $K$ for the Figure-8 laser can be expressed as

$$K = \frac{G}{4}\phi_{\text{nl}}^2 \frac{h\nu A_{\text{eff}}}{P} \tag{9}$$

and the mode-locking start condition is

$$\phi_{\mathrm{nl}}^2 > \frac{4\sigma\beta}{h\nu A_{\mathrm{eff}}} P\tau. \tag{10}$$

The nonlinear phase difference for the pulse in the NALM is given by

$$\phi_{\mathrm{nl}} = \frac{\pi n_2 L P}{\lambda A_{\mathrm{eff}}}(G-1) \tag{11}$$

and the seeding pulse parameters for initiating the mode-locking process are given by

$$\frac{P}{\tau} > \frac{4\sigma\beta}{h\nu A_{\mathrm{eff}}}\left(\frac{A_{\mathrm{eff}}\lambda}{\pi n_2 L(G-1)}\right)^2. \tag{12}$$

In order to find the value of the average output power of the laser corresponding to the second threshold we take into consideration the fact that such types of lasers are analogous to lasers with fast saturable absorbers, the basic characteristics of which can be predicted from the fluctuational model [16]. In this model the laser mode-locking process starts up from CW generation. The intensity fluctuations are considered as a narrowband Gaussian noise. At the level of average intensity $\langle P_{\mathrm{CW}}\rangle$ and a number of oscillating longitudinal modes $m$ the most intensive for the cavity round-trip period spike has a peak intensity

$$\langle P_{\mathrm{fl}}\rangle = \langle P_{\mathrm{CW}}\rangle \ln m \tag{13}$$

and duration

$$\langle \tau_{\mathrm{fl}}\rangle = \frac{T}{m}\ln^{1/2} m. \tag{14}$$

By substituting (13) and (14) in (12) we obtain the value of the second threshold

$$\langle P_{\mathrm{CW}}\rangle = \frac{4\sigma\beta T}{h\nu A_{\mathrm{eff}} m \ln^{1/2} m}\left(\frac{A_{\mathrm{eff}}\lambda}{\pi n_2 L(G-1)}\right)^2. \tag{15}$$

For our laser we have $m = 3000$ and $G = 20$ (see figure 3), $\sigma = 8\times 10^{-21}$ cm$^2$, and taking $\beta = 0.8$ we obtain $\langle P_s\rangle = 20$ $\mu$W. The output power in the point of the second threshold in the figure 2 is (40 $\mu$W) that corresponds to the a power at the NALM input of about 100 $\mu$W. The discrepancy between estimated and observed mode-locking threshold may be attributed to the simplified model of the laser fluctuations. Nevertheless, this model gives a value of correct order of the second threshold power level.

### *3.4. Generation of shorter pulses*

A very important problem is ultrashort pulse generation in a fibre laser. For generation of sub-100 fs pulses one has to cut substantially the length of nonlinear loop increasing the average output power of the laser. However, in exploiting this method, one runs into several serious problems. The first one is concerned with a pump source capable of providing a rather high level of pump power (about 1 W or more). Another problem is the special requirements for the erbium-doped fibre: to ensure a nonlinear phase difference between counter-propagating waves one needs to use a short length (around 1 m) of heavily doped

fibre, which in turn gives rise to a problem concerned with the complicated behaviour of $k''$ along a doped fibre.

Finally, shortening of NALM results in not only a decrease of pulse duration but also gives rise to intracavity losses caused by the soliton self-frequency shift. Indeed, this effect manifests itself as a shift of the soliton carrier frequency $\delta\omega$ and is proportional to $\tau^{-4}$ [17]. In the present configuration it results in a moving away of the pulse central frequency from the centre of the gain bandwidth. The group velocity dispersion in the fibre translates the frequency shift into a timing shift $\delta t$. Since pulses travelling within the NALM loop have different intensity, the intensity-dependent phase shift and consequently $\delta t$ are different in the two directions, and for a given loop length pulse narrowing leads to an incomplete switch, since two counter-propagating pulses no longer completely overlap at the coupler because their unequal frequency shifts separate them spectrally and temporally. This results in a gain increase, which in turn causes spreading of the generated pulses.

There are two possible solutions to overcome these difficulties. First one can use an external signal as a seed to initiate a mode-locked process and the results of this study will be published elsewhere [18]. A second way to generate ultrashort pulses is quite obvious: since the output laser pulse is in fact a multisoliton, then with a suitable length of dispersion-shifted fibre one can achieve compression of multisoliton pulses. Indeed, when we spliced 60 m of a fibre with dispersion $D = -1.7$ ps nm$^{-1}$ km$^{-1}$ than at the output of this fibre we observed soliton pulses with duration 280 fs (figure 7($a$)) having the spectrum shown in figure 7($b$). Note the slight shift of the spectrum centre towards the 'red' wavelength due to the effect of the soliton self-frequency shift. Compression of the noise pulses was also observed (figures 7($c$) and ($d$)). The last result supports the assertion that properties of the noise pulses are similar to those of Raman soliton noise [12].

## 4. Conclusion

We have presented an experimental study of the Figure-8 laser based on co-doped Yb–Er fibre. Our results show that, depending upon pump power, the laser generates either a sequence of solitons or soliton bunches or soliton noise. We have demonstrated a simple way to produce shorter pulses through a multisoliton compression effect. A mode-locking starting condition was derived and using the fluctuation model one could roughly estimate the second threshold value.

## Acknowledgment

The authors wish to thank V V Afanasjev for valuable discussions.

## References

[1] Kafka J D, Baer T and Hall D W 1989 *Opt. Lett.* **14** 1269
[2] Davey R P, Langford N and Ferguson A I 1991 *Electron. Lett.* **27** 1257
[3] Takada A and Mijazawa A 1990 *Electron. Lett.* **26** 216
[4] Bulushev A G, Dianov E M and Okhotnikov O G 1991 *Opt. Lett.* **16** 88
[5] Duling I III 1991 *Opt. Lett* **16** 539
[6] Richardson D J, Laming R I, Payne D N, Philips M W and Matsas V J 1991 *Electron. Lett.* **27** 731
[7] Nakazawa M, Yoshida E and Kimura Y 1991 *Appl. Phys. Lett* **59** 2073
[8] Matsas V J, Newson T P, Richardson D J and Payne D N 1992 *Electron. Lett.* **28** 1391

[9] Fermann M E, Haberl F, Hofer M and Hochreiter H 1990 *Opt. Lett* **15** 752
[10] Richardson D J, Laming R I, Payne D N, Matsas V and Phillips M W 1991 *Electron. Lett.* **27** 542
[11] Grudinin A B, Richardson D J and Payne D N 1992 *Electron. Lett.* **28** 67
[12] Vodopyanov K L, Grudinin A B, Dianov E M, Kulevsky L A and Prokhorov A M 1987 *Sov. J. Quantum Electron.* **14** 2053
[13] Dianov E M, Luchnikov A V, Pilipetskii A N and Prokhorov A M 1992 *Appl. Phys.* B **54** 175
[14] Haus H A, Fujimoto J G and Ippen E P 1991 *J. Opt. Soc. Am.* B **8** 2068
[15] Ippen E P, Liu L Y and Haus H A 1990 *Opt. Lett.* **15** 183
[16] Kryukov P G and Letokhov V S 1972 *IEEE J. Quantum Electron.* **8** 766
[17] Gordon J P 1986 *Opt. Lett.* **11** 662
[18] Grudinin A B and Khrushchev I Yu 1993 *Electron. Lett.* in press